Unmasking Electronic Energy Transfer of Conjugated Polymers by Suppression of O_2 Quenching

Ji Yu, Dehong Hu, Paul F. Barbara*

The photochemistry of poly[2-methoxy, 5-(2′-ethyl-hexyloxy)-*p*-phenylene-vinylene] (MEH-PPV) has been found to be highly dependent on the presence of O_2, which increases singlet exciton quenching dramatically. Spectroscopy on isolated single molecules of MEH-PPV in polycarbonate films that exclude O_2 reveals two distinct polymer conformations with fluorescence maxima near 555 and 580 nanometers wavelength, respectively. Time-resolved single-molecule data demonstrate that the 580-nanometer conformation exhibits a "landscape" for intramolecular electronic energy relaxation with a "funnel" that contains a 580-nanometer singlet exciton trap at the bottom. The exciton traps can be converted to exciton quenchers by reaction with O_2. Conformationally induced, directed-energy transfer is arguably a critical dynamical process that is responsible for many of the distinctive photophysical properties of conjugated polymers.

The fluorescence of conjugated polymers (*1–3*) is heavily influenced by the conformations of the polymer chains (*4–7*). Recent experiments on the spectroscopic anisotropy of single conjugated polymer molecules (*8, 9*) reveal an ordered, collapsed conformation with many parallel chain-chain contacts. A detailed understanding of the spectroscopic and photophysical consequences of conformational structure has been difficult to establish experimentally due to the tremendous heterogeneity of conjugated polymers. Single-molecule spectroscopy (SMS) allows the properties of individual molecules to be deduced despite their presence within a highly heterogeneous environment (*10–14*). Applications of SMS to conjugated polymers have focused on fluorescence intensity fluctuations that result primarily from photochemically induced quenchers that thermalize the exciton energy and lead to "dark states" (*15*). This approach has led to qualitative information on the electronic energy transfer mechanism of conjugated polymers. Little information, however, has been obtained about the role of conformational structure in the energy transfer mechanism where excitons may move or may localize in traps before emitting.

We present SMS results for MEH-PPV (*16*) that represent a greater than two order of magnitude improvement in signal-to-noise compared with previous measurements (*8*) that allows for a precise determination of the fluorescence spectrum and its temporal evolution on the picosecond and slower time scale. The improvement is due to a longer averaging time, which have been made possible by a greatly improved sample preparation technique (*17*) that diminishes the rate of photo-alteration due to photo-oxidation during the averaging (acquisition) process for each MEH-PPV molecule. By excluding O_2, we avoid permanent changes to the intrinsic photochemistry. The emission spectra of two typical MEH-PPV molecules (Fig. 1B) were recorded under conditions of low excitation intensity and rigorous O_2 depletion that effectively suppresses spectral distortion due to photochemistry and other photoinduced processes, such as intensity fluctuation due to photo-generated quenchers. The ensemble fluorescence spectrum (Fig. 1A) of ~80 molecules of MEH-PPV isolated in an inert thin-film polymer (polycarbonate) host reveals the typical band shape of a conjugated polymer. The single-molecule fluorescence spectra of MEH-PPV are significantly narrower than the ensemble spectrum (Fig. 1A) in polycarbonate, but comparable in width to the ensemble spectrum in liquid toluene.

The ensemble distribution of the fluorescence spectral maxima (λ_{max}) of single molecules (Fig. 2A) exhibits a surprising double-peaked distribution with two maxima (560 and 580 nm). Similar double-peaked distributions were observed in other polymer hosts, but with slightly different maxima (553 and 583 nm in polymethylmethacrylate and 555 and 575 nm in polystyrene). The presence of two distinct peaks in the spectral maxima distribution indicates that two different types of conformations of MEH-PPV are trapped in the polymer host matrix. This result is surprising because a broad, continuous distribution would be expected for a polymer molecule with so many conformational degrees of freedom.

In order to further interpret the spectral distribution in Fig. 2, we note that the absorption and fluorescence of conjugated polymers involve quasi-localized chromophores on the polymer chain (*18–20*). For our sample, there are about 2000 repeat units for each MEH-PPV molecule. Each singlet optical excitation (exciton) is shared by about 10 adjacent repeat units (*21*), so there are ~200 chromophores in a single molecule. Absorption of photons near the absorption peak wavelength (~500 nm) of the vibronically broadened spectrum randomly excites the different localized chromophores. Under the relatively low excitation conditions of these experiments, only one singlet exciton is present in the molecule during the excited state lifetime (~300 ps) (*22, 23*). Evidence suggests that intramolecular electronic energy transfer (*8, 15, 24*) converts the mobile excitons to

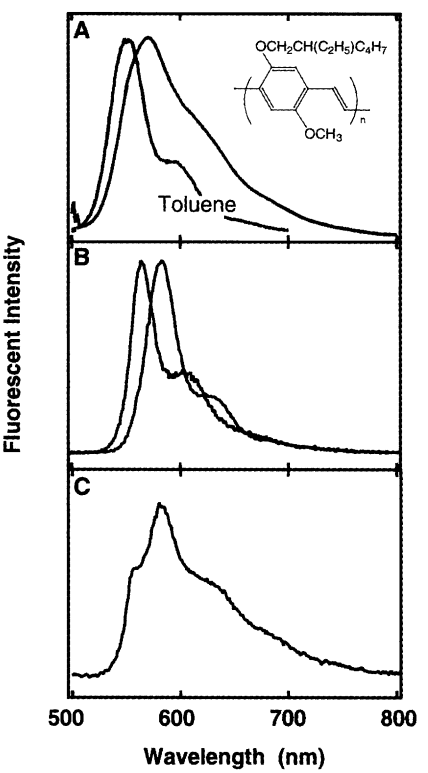

Fig. 1. (**A**) The "ensemble" fluorescent spectrum of MEH-PPV in a pure liquid toluene solution (left peak) and in a polycarbonate matrix at ambient temperature (right peak). The spectrum in polycarbonate matrix was constructed by summing up single-molecule spectra for ~80 MEH-PPV molecules. The inset shows the chemical structure of MEH-PPV. (**B**) Typical single-molecule spectra of MEH-PPV peaked at 560 and 580 nm, respectively. (**C**) A single-molecule spectrum of MEH-PPV that has a "mixed" feature of both a 560-nm peak and a 580-nm peak.

Department of Chemistry and Biochemistry, University of Texas, Austin, TX 78712, USA.

*To whom correspondence should be addressed. E-mail: p.barbara@mail.utexas.edu

trapped excitons that are located at one or more low-transition-energy regions (or exciton traps) on a time scale shorter than the excited state lifetime. Thus, the fluorescence spectra tend to reflect the spectral properties of the exciton traps rather than the typical chromophore along the chain. It is important to note that the exciton trapping process does not quench the fluorescence of MEH-PPV, because the mobile and trapped excitons have similar fluorescence quantum yields and emission lifetimes.

Some insight into MEH-PPV conformations, and possible structures for exciton traps, can be found in recent simulations of stiff polymer chains with tetrahedral chemical defects (*9*). Conjugation imparts stiffness to polymer chains. Tetrahedral defects are the results of incomplete elimination during the final step in the synthesis of MEH-PPV. Simulations predict that two distinct conformations can form depending on the strength of the intrachain interactions. Intrachain interactions can be tuned by varying the solvent environment around the chain. Typical structures from these simulations are shown in Fig. 2C (*9*). One conformation is the defect cylinder, which is an ordered collapsed form that is predicted to exhibit a significant single-molecule excitation anisotropy ($<M^2>^{1/2}$ = 0.46) because of the parallel orientation of the chains (*9*). The other conformation, the defect coil, is predicted to be less anisotropic ($<M^2>^{1/2}$ = 0.28) and involves rod-like segments of the polymer connected by tetrahedral defects in the polymer chain. The conversion of the defect coil to the defect cylinder resembles a phase transition (*9*) due to cooperative nature of intramolecular chain-chain interactions (*25–28*). Qualitatively, the simulations suggest that the defect coil and defect cylinder have similar conjugation lengths since they appear from the typical structure (Fig. 2C) to be controlled by the distribution of tetrahedral defects rather than the chain conformation. In contrast, the simulation predicts much more π-π intrachain interactions for the defect cylinder.

We used methods described in Hu *et al.* (*9*) to measure $<M^2>^{1/2}$ of the red and blue conformations of MEH-PPV in PMMA films. The resultant values (0.46 and 0.44, respectively) suggest that both forms should be assigned to the collapsed defect-cylinder structure. Considering this likely defect-cylinder structure, a good candidate for the exciton traps in the red-shifted, 580-nm conformation of MEH-PPV would be chain-chain contacts that are sufficiently close to produce a significant lowering of localized transition energy through exciton interactions between nearby parallel oriented chromophores, such as in molecular aggregates (*29*). In the case of conjugated polymer, model compounds with nearby parallel chain contact produce a red shift and broadening due to excimer-like interactions (*30*). For the MEH-PPV 580-nm conformation, the absence of excimer broadening may simply result from a failure to obtain the precise spatial alignment of molecular orbitals that are necessary for an excimer interaction. A chain segment with an extended conjugation length could also be responsible for the 580-nm trap. This possibility seems unlikely, however, because the variation in spectral maxima versus conjugation length is relatively small for long conjugation lengths according to theory and results for model compounds (*19, 24*).

To be consistent with the data, the conformational feature responsible for the 580-nm exciton trap would have to be relatively energetically unfavorable in the ground state of MEH-PPV, because the blue form of MEH-PPV appears to contain few, if any, of these contacts. A careful examination of the spectra of individual MEH-PPV molecules reveals, however, the presence in many cases of both red- and blue-emitting spectral components (Fig. 1C). That may reflect incomplete energy transfer to the longest wavelength exciton traps, as described below.

The fluorescence spectrum of MEH-PPV in a dilute toluene solution (Fig. 1A) is extremely sharp and centered at 555 nm near the emission maxima of the blue-emitting form in the film (Fig. 2B). Light-scattering studies in *p*-xylene, which is a similar solvent to toluene, measure a radius of gyration (52.4 nm) and hydrodynamic radius (35.9 nm) for MEH-PPV (*31*) suggestive of a defect-coil structure that almost definitely lacks close chain-chain contacts. Because MEH-PPV in pure toluene (the solvent used for spin-coating) is apparently in the defect-coil conformation, the chain collapse must occur late in the spin-coating process when the relative amount of polycarbonate to toluene is increasing in the environment of MEH-PPV.

The enhancement in MEH-PPV single-molecule stability we now report allowed us to investigate the role of conformational structure in the photochemistry of a conjugated polymer. Under the extremely low oxygen concentration of our sample, MEH-PPV molecules exhibit a time-independent fluorescence intensity and spectral band shape (under low-intensity excitation; Fig. 3A). The "sudden" fluorescence fluctuations (to a lower intensity level), which are analogous to previous observations, are assigned to a reversibly formed, photochemically generated

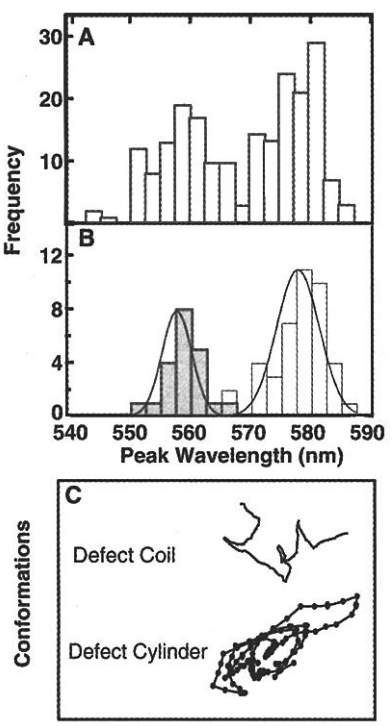

Fig. 2. (**A**) Distribution of the peak wavelength (λ_{max}) of single-molecule fluorescent spectra of MEH-PPV found by simply finding the maxima in spectra analogous to Fig. 1B. Histogram was constructed from data of several different samples using the same sample preparation procedure. (**B**) Two histograms plotted in different shades, which represent data taken from two different areas in the same sample film. (**C**) "Snapshot" of the defect-coil conformation and defect-cylinder conformation of a single polymer chain (*9*).

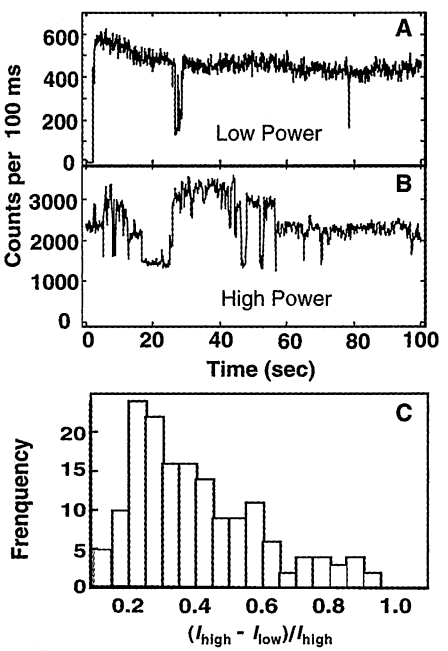

Fig. 3. (**A**) A fluorescence intensity transient of a single MEH-PPV molecule under continuous-wave (cw) irradiation at 488 nm. (**B**) A similar intensity transient from the same molecule as in (A), but with an irradiation power six times higher. (**C**) A histogram of fluorescent quenching depths for different single MEH-PPV molecules in the ensemble. I_{high} denotes the fluorescence intensity of unquenched molecule and I_{low} is the intensity after a quenching event happened. Intensity jumps smaller than 10% (primarily due to noise) were discarded in constructing the histogram.

fluorescence quencher on the polymer chain (*8, 15*). Thus, the rate of forming the fluorescence quencher depends strongly on oxygen concentration. A possible chemical structure for the fluorescence quenchers is an O_2/polymer adduct with charge transfer character: polymer$^+$/O_2^-. Electron deficiencies (such as radical cations) are effective quenchers in conjugated molecules (*32*). The strong dependence of the rate of formation of quenchers on the excitation rate (Fig. 3B) suggests that O_2 is reacting with excitons [probably triplets (*33, 34*)] to form the quenchers. The regular and reproducible events of quenching strongly suggest that the fluorescence quenchers are being formed repeatedly at the same site on the polymer chain. In previous single-molecule studies on conjugated polymers, high O_2 concentrations led to the formation of multiple quenchers, resulting in complex spectral dynamics and rapid permanent photo-oxidation (*8, 15*).

The position of the fluorescence quencher along the polymer chain is apparently dictated by S_1 exciton migration. This process "funnels" excitons to exciton traps, which react with O_2 to form the quencher. This "energy funneling" is presumably a result of the ordered regions of the polymer chain containing parallel chains. These regions should favor rapid, directional energy transfer by resonance energy transfer due to aligned transitions dipole moments and short chromophore energy-transfer distances. The quenching depths for an "individual intensity level" represent the fraction of initial excitons that are funneled to a specific quencher. The energy migration corresponds to a "funnel" associated with the folded portion of the polymer. The unquenched emission in a molecule that already contains one quencher may be due to either (i) chromophores not associated with an effective energy funnel or (ii) excitons in a different funnel than the one that contains the quencher. A typical molecule exhibits two or three intermediate intensity levels, which suggests that multiple funnels are present. This system of energy funnels can be envisaged as forming a "landscape for intramolecular electronic energy transfer." The ensemble distribution of quenching depths (Fig. 3C) shows that the most probable quenching depth is more than 20%, whereas the upper limit is almost 100% of the molecule. The large variation of the quenching depths is not unexpected because of the broad conformational and molecular weight distribution in the ensemble.

Evidence that low transition energy exciton traps are involved in the energy funnels is presented in Fig. 4. Fluorescence spectra and picosecond time-resolved emission transients recorded during the intensity fluctuation process have been sorted into spectra (Fig. 4B) and picosecond transients (Fig. 4C) for the "fully on" [unphotolyzed (**U**) state] and for the "intermediate intensity level" [photolyzed (**P**) state]. The **P** state exists during the presence of a reversibly formed quencher. For the molecule studied in Fig. 4B, the cumulated **U** spectrum is predominantly red emission with a small portion of blue-edge emission. The difference spectrum (**U** – **P**) is exclusively sharp, red-shifted emission, which suggests that energy transfer is extremely rapid and efficient within the collapsed region of the molecule. Thus, when a quencher is formed in this region, the emission is quenched by efficient funneling of S_1 excitons to the lowest energy chromophores. Indeed, the extraordinarily sharp and red-shifted emission in the **U** – **P** difference spectrum (Fig. 4D) demonstrates that nearly 30% of the excited repeat units (~600 repeat units) all rapidly channel their S_1 excitons to a exciton trap that has a narrow red-shifted emission. The extraordinarily narrow emission spectrum suggests that very few chromophores, perhaps even one chromophore, is responsible for the **U** – **P** spectrum. The reproducibility of the **U** and **P** spectra during several quenching cycles demonstrates that while the quencher is repeatedly being formed and destroyed, the underlying conformationally induced "funnel" structure for exciton migration is permanent on these time scales.

The picosecond time-resolved data (on a similar MEH-PPV single molecule) is also highly suggestive of rapid and efficient funneling of S_1 excitons to quenchers. The presence of photoinduced quenching is especially apparent at early times in the time resolved emission transients (Fig. 4C). The 30% decreased $t = 0$ fluorescence intensity in the **U** – **P** data is assigned to quenching on a time scale much shorter than our instrument response function (~50 ps). This result implies that significant amount of the initially excited chromophores are associated with excitons that are transferred to the quencher in a time scale much less than 50 ps. Measurements on a few of the single molecules reveal evidence of energy transfers (quenching) on time scale as long as 100 ps. This result suggests slow and inefficient energy transfer, perhaps in molecules with less conformational order.

The SMS data of MEH-PPV suggest a molecular interpretation of conjugated polymer aggregation. Aggregation, which is a critical factor in the performance of neat conjugated polymer film in display devices and organic thin-film lasers, has been attributed to chain-chain interactions (*4, 5*). Conjugated polymer aggregation is usually associated with a red-shifted emission, a broadening of the emission spectrum, a loss in fluorescence quantum yield, and a nonexponential fluorescence decay. Although the collapsed single-molecule chains reported herein do indeed exhibit a red-shifted emission, the spectra are relatively sharp. In addition, the time-resolved single-molecule fluorescence dynamics lacks the nanosecond decay component (*35*) associated with aggregation (Fig. 4C) and suggests that interchain rather than intrachain interactions are required for MEH-PPV aggregation effects. A similar conclusion was recently reached by T. Q. Nguyen and coworkers based on bulk spectroscopic data (*5*).

In closing, it is interesting to speculate to what extent the conclusions presented here for polymer-matrix isolated MEH-PPV molecules also apply for pure MEH-PPV films. For equilibrium pure polymer samples, a collapsed polymer structure is not usually expected because a polymer is a

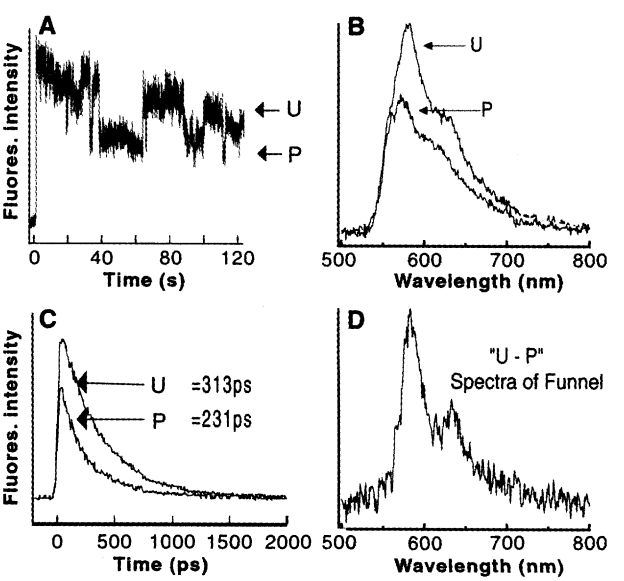

Fig. 4. (**A**) The time-dependent fluorescence intensity of a single MEH-PPV molecule undergoing intensity fluctuations due to quenchers induced by excitation at 470 to 480 nm with a frequency-doubled Ti:sapphire laser (repetition rate = 76 MHz). Similar transients are observed for cw excitation (488 nm) as in Fig. 3. (**B**) "Sorted" single-molecule fluorescent spectra of the **U** and **P** states. (**C**) Sorted single-molecule time-resolved kinetic traces of the **U** and **P** states, recorded by the time-correlated single-photon counting technique with a microchannel plate detector. Lifetimes (τ) were obtained for each trace by single-exponential fitting. (**D**) The difference (**U** – **P**) between the **U** and **P** emission spectra.

good solvent for itself. However, conjugated polymer films are typically prepared by spin coating, which may kinetically trap nonequilibrium ordered collapsed conformations. The presence of such structure could account for the experimentally observed local chain-chain order and anisotropy of such films (*36, 37*). However, such order could also be produced by parallel packing of chains from different polymer molecules (*5*). Indeed, both types of chain-chain packing may compete in the highly heterogeneous and variable morphologies of conjugated polymer thin films.

References and Notes

1. R. H. Friend *et al.*, *Nature* **397**, 121 (1999).
2. F. Hide, M. A. Diazgarcia, B. J. Schwartz, A. J. Heeger, *Acc. Chem. Res.* **30**, 430 (1997).
3. T. M. Swager, *Acc. Chem. Res.* **31**, 201 (1998).
4. R. Jakubiak, C. J. Collison, W. C. Wan, L. J. Rothberg, B. R. Hsieh, *J. Phys. Chem. A* **103**, 2394 (1999).
5. T. Q. Nguyen, V. Doan, B. J. Schwartz, *J. Chem. Phys.* **110**, 4068 (1999).
6. H. Sirringhaus *et al.*, *Nature* **401**, 685 (1999).
7. R. Österbacka, C. P. An, X. M. Jiang, Z. V. Vardeny, *Science* **287**, 839 (2000).
8. D. Hu, J. Yu, P. Barbara, *J. Am. Chem. Soc.* **121**, 6936 (1999).
9. D. Hu *et al.*, *Nature* **405**, 1030 (2000).
10. W. E. Moerner and M. Orrit, *Science* **283**, 1670 (1999).
11. S. Weiss, *Science* **283**, 1676 (1999).
12. X. S. Xie and J. K. Trautman, *Annu. Rev. Phys. Chem.* **49**, 441 (1998).
13. T. Basche, W. E. Moerner, M. Orrit, U. P. Wild, *Single Molecule Optical Detection, Imaging, and Spectroscopy* (Verlag Chemie, Munich, 1996).
14. R. Rigler, *J. Biotechnol.* **41**, 177 (1995).
15. D. A. Vandenbout *et al.*, *Science* **277**, 1074 (1997).
16. The single-molecule spectra were acquired at ambient temperature using a previously described sample scanning confocal apparatus. Typical conditions for the single-molecule spectra we describe here are excitation spot size = 320 nm, excitation wavelength = 488 nm, and excitation power = 100 nW. The MEH-PPV sample used in the paper was supplied by Uniax Corp.
17. Single-molecule samples were prepared by spin-coating a toluene solution containing 10^{-7} g/ml of MEH-PPV and 10 mg/ml polycarbonate onto a glass substrate. The procedure prepared a film of 500 ± 100 nm thickness. To reduce the O_2 concentration, a freshly spin-coated film was exposed to vacuum (1.0×10^{-5} Pa) for 30 min, and then coated with a 200-nm-thick evaporated Al overlayer in order to seal the film from atmospheric O_2.
18. H. Bassler and B. Schweitzer, *Acc. Chem. Res* **32**, 173 (1999).
19. S. Mukamel, S. Tretiak, T. Wagersreiter, V. Chernyak, *Science* **277**, 781 (1997).
20. A. Kohler *et al.*, *Nature* **392**, 903 (1998).
21. H. Meier, U. Stalmach, H. Kolshorn, *Acta Polym.* **48**, 379 (1997).
22. L. Smilowitz, A. Hays, A. J. Heeger, G. Wang, J. E. Bowers, *J. Chem. Phys.* **98**, 6504 (1993).
23. I. D. W. Samuel *et al.*, *Synth. Met.* **84**, 497 (1997).
24. G. Padmanaban and S. Ramakrishnan, *J. Am. Chem. Soc.* **122**, 2244 (2000).
25. A. Y. Grosberg, *Biophysics* **24**, 30 (1979).
26. Y. A. Kuznetsov and E. G. Timoshenko, *J. Chem. Phys.* **111**, 3744 (1999).
27. H. Noguchi and K. Yoshikawa, *J. Chem. Phys.* **109**, 5070 (1998).
28. Y. Q. Zhou, M. Karplus, J. M. Wichert, C. K. Hall, *J. Chem. Phys.* **107**, 10691 (1997).
29. V. Czikkley, H. D. Försterling, H. Kuhn, *Chem. Phys. Lett.* **6**, 11 (1970).
30. G. Bazan *et al.*, *J. Am. Chem. Soc.* **120**, 9188 (1998).
31. C. L. Gettinger, A. J. Heeger, J. M. Drake, D. J. Pine, *J. Chem. Phys.* **101**, 1673 (1994).
32. J. Seth *et al.*, *J. Am. Chem. Soc.* **116**, 10578 (1994).
33. R. Osterbacka, M. Wohlgenannt, D. Chinn, Z. V. Vardeny, *Phys. Rev. B* **60**, R11253 (1999).
34. G. D. Hale, S. J. Oldenburg, N. J. Halas, *Phys. Rev. B* **55**, 16069 (1997).
35. M. Yan, L. J. Rothberg, E. W. Kwock, T. M. Miller, *Phys. Rev. Lett.* **75**, 1992 (1995).
36. J. W. Blatchford *et al.*, *Phys. Rev. B* **54**, R3683 (1996).
37. C. Y. Yang, F. Hide, M. A. Diazgarcia, A. J. Heeger, Y. Cao, *Polymer* **39**, 2299 (1998).

38. Supported by grants from NSF and the Robert A. Welch Foundation.

16 February 2000; accepted 28 June 2000

Calcium-Aluminum–Rich Inclusions from Enstatite Chondrites: Indigenous or Foreign?

Yunbin Guan,[1] Gary R. Huss,[2,3] Glenn J. MacPherson,[1] Gerald J. Wasserburg[2]

The primary mineral assemblages and initial $^{26}Al/^{27}Al$ ratios of rare calcium-aluminum–rich inclusions (CAIs) from enstatite (E) chondrites are similar to those of CAIs from other chondrite classes. CAIs from all chondrite classes formed under oxidizing conditions that are much different from the reducing conditions under which the E chondrites formed. Either CAIs formed at an earlier, more oxidizing epoch in the region where E chondrites ultimately formed, or they formed at a different place in the solar nebula and were transported into the E chondrite formation region.

CAIs are refractory objects that make up <5 volume percent of primitive chondritic meteorites [e.g., (*1*)]. They were among the first objects formed in the solar nebula ~4.56 billion years ago and therefore bear important physical and chemical information about the earliest stages of solar system evolution. Previous studies demonstrated that CAIs carry excesses of ^{26}Mg compared with the average solar system Mg (*2*, *3*). These ^{26}Mg excesses correlate with the Al/Mg ratios of the host minerals within individual CAIs and therefore are due to in situ decay of the short-lived radionuclide ^{26}Al [half-life ($t_{1/2}$) ~730,000 years] that was present in the inclusions when they formed. Voluminous data for CAIs in carbonaceous (C) chondrites (*4*) establish a canonical initial abundance ratio, $(^{26}Al/^{27}Al)_o$, for the early solar system of $\sim 5 \times 10^{-5}$. CAIs in ordinary (O) chondrites share this same initial ratio (*5*). However, some rare CAIs from C and O chondrites formed with little or no ^{26}Al. Either those inclusions formed several million years after most CAIs (i.e., after ^{26}Al had largely decayed), or ^{26}Al was heterogeneously distributed in the early solar system.

CAIs from C and O chondrites share similar mineral assemblages and distinctive oxygen isotopic features, raising the possibility that CAIs might have formed in a single restricted region of the solar nebula (*6*). A way to test this interesting possibility is to study CAIs from E chondrites. E chondrites have distinctive mineral assemblages that could only have formed under reducing conditions (*7*), and they may have formed in a different region of the solar nebula than C and O chondrites. If CAIs in E chondrites share this distinctive reduced mineral assemblage and yet share the isotopic characteristics of CAIs in C and O chondrites, this would indicate that refractory objects formed in many different nebular locales from broadly similar isotopic reservoirs. Such a result would support the idea that ^{26}Al was widely distributed in the early solar nebula. Alternatively, if CAIs in E chondrites are mineralogically similar to CAIs in C and O chondrites and lack the extremely reduced phases of the host E chondrites, this would imply that all CAIs formed under similar conditions, perhaps in a single region from which they were broadly distributed.

Here, we report the results of a systematic search for and Mg-isotopic analysis of CAIs in 26 polished thin sections of 14 unequilibrated E chondrites. Seventy-two CAIs >10 μm across and eight isolated hibonite and spinel mineral fragments were identified by x-ray area mapping of the thin sections (Table 1). These inclusions were studied by scan-

[1]Department of Mineral Sciences, National Museum of Natural History, Smithsonian Institution, Washington, DC 20560–0119, USA. [2]Lunatic Asylum, Division of Geological and Planetary Sciences 170-25, California Institute of Technology, Pasadena, CA 91125, USA. [3]Department of Geology and Center for Meteorite Studies, Arizona State University, Tempe, AZ 85287–1404, USA.